

## Short-range order and energetics of disordered silicon-carbon alloys

P. C. Kelires

*Physics Department, University of Crete, 71110 Heraklion, Crete, Greece  
and Research Center of Crete, 71110 Heraklion, Crete, Greece*

(Received 17 April 1992)

Monte Carlo simulations, based on an empirical potential approach, have yielded detailed information about the structural and compositional short-range order as well as the energetics of disordered silicon-carbon alloys. It is found that the network of the amorphous phase deviates from an ideal tetrahedral geometry because a considerable number of carbon atoms are threefold coordinated, especially in the carbon-rich samples. Silicon, on the other hand, retains a coordination number of four. There is no phase separation. Comparing the present results with experimental observations, it is speculated that hydrogenation will promote tetrahedral carbon coordination. In the liquid phase the tendency of carbon towards low coordination dominates the structural characteristics. Silicon coordination in stoichiometric samples is much less than in pure *l*-Si, indicating persistence of tetrahedral order and covalent bonding. Even at high pressures ( $\sim 1$  Mbar) carbon coordination remains lower than four, while at this pressure pure *l*-C is less dense than diamond. Regarding chemical ordering, the two disordered phases show a characteristic difference. The amorphous samples exhibit a significant degree of ordering (but with homopolar bonds always present), while the liquid has a random distribution of Si and C atoms. This gradual weakening of the Si—C bond is nicely explained by analyzing the total energy of the system into bond energies. The bulk modulus of the amorphous phase is found to be larger than that of *c*-SiC.

### I. INTRODUCTION

Interest in the properties of disordered semiconductor alloys is growing continuously, not only because of technological applications but also because of fundamental and fascinating questions to which they give rise. It is not surprising then that theoretical investigations of such systems have been intense in recent years. Particular attention is given to the nature of the amorphous and liquid states at the microscopic level. Nevertheless, the complexity of structural properties exhibited by these highly disordered phases makes their study difficult and quite challenging. Very often, microscopic descriptions are given based on arguments derived by analogy to the better understood crystalline state, or by applying statistical methods in order to model the experimental results. Such approaches, though very useful in obtaining qualitative descriptions, are rather inadequate to deal with the subtle and sometimes unexpected phenomena which are introduced by structural disorder.

The fundamental issue to be dealt with, when studying disordered phases, is the specification of the network topology that defines the way the atomic sites are interconnected with each other. Theories of electronic states in disordered systems depend inescapably on a reliable description of the overall topology. When discussing the amorphous state, a complete description of the structure requires the knowledge of both the short-range order (SRO), defined as the local atomic arrangement about a given reference atom, as well as of medium-range order (MRO), related to the distribution of dihedral angles and the resulting ring statistics.<sup>1</sup> Long-range order (LRO) and periodicity are, of course, lacking in amorphous materials. The degree of MRO signifies the remnants of

crystalline order in the amorphous state and it can even be absent in heavily disordered systems. SRO is always present and is specified by the number of nearest neighbors, their separation from the reference atom, and their bond-angle distributions.

By interpreting experimental observations various models have been constructed in order to describe amorphous solids. The widely accepted model for the structure of elemental amorphous semiconductors, such as  $\alpha$ -Si or  $\alpha$ -Ge, is the continuous random network (CRN) model proposed by Polk.<sup>2-4</sup> Similar models have been proposed by other workers.<sup>5,6</sup> In a random network structure the number of nearest neighbors of every atom is such that satisfies the atom's chemical valence. Thus, for  $\alpha$ -Si or  $\alpha$ -Ge, the Polk model requires that each atom has four neighbors arranged in a tetrahedral geometry. Bond lengths are distributed about their crystalline values with deviations of a few percent from the average value. Similarly, bond angles are distributed about the tetrahedral angle of  $109^\circ$  with average deviations of  $\sim \pm 10^\circ$ . Randomness in the network results from a statistical distribution of dihedral angles. Atoms are allowed to form odd-membered rings, besides the sixfold rings characteristic of the diamond structure.

In an amorphous heteropolar compound the random character of the network still holds. However, the specification of SRO is now more complicated because one needs to know not only the number of nearest neighbors, but also their type. For binary alloys which have only unlike-atom bonds in the crystalline state (like GaAs), it is now possible to have, in addition, like-atom bonds. This constitutes a new type of disorder. Interest is focused, not only on the effects of bond-length and bond-angle distortions, but also in the effects of like-atom

bond clustering configurations and the fraction of homopolar bonds, which strongly affect the electronic properties of the amorphous phase.<sup>7</sup> On the other hand, disordered bulk semiconductor alloys which have a random distribution of the atomic species in the crystal (a prototypical example is SiGe) are obviously expected to show more or less the same behavior in the amorphous phase. In all above cases, it is essential to maintain tetrahedral-like local environment throughout the solid.

An interesting possibility for a modified picture seems to be offered by amorphous semiconductor alloys containing carbon. The ability of this element to display twofold ( $sp$ ), threefold ( $sp^2$ ), and fourfold ( $sp^3$ ) coordination in a variety of materials opens up a wide range of fascinating questions about the network topology. Such a prototypical disordered alloy containing carbon is amorphous silicon carbide ( $\alpha$ -Si<sub>1-x</sub>C<sub>x</sub>). There are mainly two important reasons to why this is a fundamentally interesting compound, and they are based on the following arguments. First, the constituent elements Si and C exhibit a remarkably different behavior in their amorphous state. As discussed above,  $\alpha$ -Si is perfectly tetrahedral, being described by the Polk model. Any miscoordinated atoms, i.e., threefold- or fivefold-coordinated<sup>8</sup> atoms, must be viewed as intrinsic defects, and not as part of the inherent glassy disorder. On the other hand,  $\alpha$ -C is predominantly a threefold-coordinated ( $sp^2$ ) material, with the fraction of tetrahedral ( $sp^3$ ) atoms ranging from 1% to ~20%.<sup>9-12</sup> Dense, diamondlike  $\alpha$ -C structures with a high percentage of  $sp^3$  atoms could exist (depending on the preparation conditions, i.e., low temperature and high pressure),<sup>13,14</sup> but these are rather metastable.<sup>15</sup> Besides, it is argued that diamondlike dense phases could as well be composed of graphiticlike ( $sp^2$ ) geometries.<sup>15-17</sup> Thus, a variety of bonding possibilities might take place in an amorphous mixture of these two elements, giving rise to deviations from a tetrahedral geometry, contrary to the perfectly fourfold-coordinated zinc-blended (ZB) *c*-SiC. The degree of structural disorder will depend on the growth conditions during a given preparation method.

The second point of interest concerns the question of chemical ordering, i.e., the predominance or not of heteronuclear bonding, in the amorphous state. ZB *c*-SiC has a large negative enthalpy of formation ( $\Delta H < 0$ ),<sup>18-21</sup> which entirely favors the Si-C bond. In contrast, *c*-SiGe is a prototypical semiconductor random alloy, because the random distribution of atoms has lower energy than the ZB structure,<sup>19</sup> though both have a small positive enthalpy of formation ( $\Delta H > 0$ ), which drives the compound into phase separation at sufficiently low temperatures.<sup>19,22-24</sup> Given these observations, it will be of interest to examine if any deviations from complete chemical ordering in the amorphous phase of SiC is related to the structural disorder due to nontetrahedral arrangements of atoms, and to study the dependence of the Si-C bond strength on such disordered environments.

Liquid mixtures of Si and C pose great challenges to theoreticians as well, not only because of the expected high degree of disorder, but also because these two elements show an intriguing characteristic difference in the

elemental liquid states. In particular, liquid silicon shows metallic behavior and a rather low coordination number of ~6.4,<sup>25</sup> while most liquid metals have coordinations of ~12. On the other hand, though recent optical and dc conductivity experiments<sup>26</sup> conclude that liquid carbon at low pressure is metallic, theoretical calculations<sup>11,27</sup> indicate a very low coordination number of ~2.8, even lower than in graphite. This behavior of carbon is in sharp contrast to the behavior of Si and other group-IV elements upon melting, which exhibit increased coordination and a density increase of ~10%.<sup>28</sup> If carbon would follow this trend then *l*-C (at low *P*) should have a macroscopic density at least larger than that of graphite (2.27 gcm<sup>-3</sup>), but this is not supported by experimental studies which, instead, indicate densities less than 2.0 gcm<sup>-3</sup>.<sup>29</sup> This marked difference suggests that in a liquid mixture of these two elements there is a possibility of fascinating competing phenomena. The SRO is expected to be quite different than in a liquid alloy which is composed of elements with similar behavior, such as *l*-SiGe. Relevant questions to be answered are in what extent the presence of carbon modifies the characteristics of *l*-Si and vice versa, the existence or not of chemical ordering, and what are the properties of *l*-Si<sub>1-x</sub>C<sub>x</sub> at high pressures.

In this paper, I make a comparative study of the amorphous and liquid states of Si-C alloys, and I address various questions about SRO, such as those put forward above. Shorter reports on the properties of amorphous and liquid SiC have been recently given in separate publications.<sup>30,31</sup> The investigations are carried out using the Monte Carlo (MC) method in combination with an empirical potential in order to model the interatomic interactions. This methodology is a type of direct simulation, without any input from experiment. In this kind of approach, which is proved very useful, one avoids any *a priori* assumptions about the network topology, something which is inherent and unavoidable when trying to interpret experimental observations with statistical models. Of course, a reliable description of the interatomic interaction and energetics is essential in order to understand, and even to predict the behavior of disordered phases in the microscopic level. The development in recent years of reliable empirical interatomic potentials for semiconductors<sup>11,32-37</sup> and of *ab initio* molecular dynamics methods (Car-Parinello),<sup>38</sup> has greatly contributed to this effort. As a result, we are now in a better position to understand the properties of the amorphous and liquid states of semiconductor compounds.

In addition to their fundamental importance,  $\alpha$ -Si<sub>1-x</sub>C<sub>x</sub> films are also promising materials for technological applications, especially as *p*-doped window layers in heterojunction solar cells,<sup>39,40</sup> or as wide-band-gap intrinsic layers in multilayer  $\alpha$ -Si solar cells.<sup>41</sup> They are grown by a variety of methods, such as plasma chemical vapor deposition (CVD),<sup>42</sup> glow discharge decomposition of silane and hydrocarbons,<sup>43</sup> and reactive sputtering of silicon in an atmosphere of hydrocarbons.<sup>44,45</sup> The samples grown by these methods usually contain an appreciable amount of hydrogen, ranging from 10 to 40%, which is found to depend on the carbon content. Unhydrogenated samples are prepared either by reactive sputter-

ing in an argon atmosphere<sup>45,46</sup> or by evaporation of crystalline SiC in vacuum.<sup>47</sup>

Studies of these films, both hydrogenated and unhydrogenated, by a variety of experimental techniques have been extensive.<sup>44–48</sup> However, several characteristic properties and central questions about SRO remain controversial. These include the ratio of threefold ( $sp^2$ ) to fourfold ( $sp^3$ ) carbon sites, the existence or not of chemical ordering, whether carbon and silicon atoms are mixed homogeneously or whether there is phase separation, and how hydrogenation influences coordination. As an indication of the conflicting descriptions given by experiment, we mention the following. Direct evidence for homonuclear bonds in sputtered  $\alpha$ -SiC is provided by Gorman and Solin.<sup>46</sup> Their Raman spectra clearly show the existence of both graphitelike and diamondlike bonds in carbon-deficient ( $Si_{0.59}C_{0.41}$ ) samples, where such bonds are less likely to occur. However, infrared-absorption measurements in sputtered films by Fagen<sup>49</sup> have been interpreted as indicating a very small number of homonuclear bonds. Regarding carbon coordination, the presence of a strong  $\pi^*$  peak in the electron energy-loss spectra (EELS) of evaporated  $\alpha$ -SiC by McKenzie, Berger, and Brown<sup>47</sup> directly indicates the existence of threefold-coordinated carbon. Yet, electron diffraction results in the same material are interpreted as indicating a predominantly tetrahedral network.<sup>50</sup> Also, extended x-ray-absorption (EXAFS) and electron energy-loss fine-structure (EXELFS) measurements on sputtered  $\alpha$ -SiC by Kaloyeros, Rizk, and Woodhouse<sup>45</sup> indicate fourfold C coordination and almost complete chemical ordering. Similar conclusions are drawn about hydrogenated samples too.<sup>45,48</sup>

Here, as a natural starting point, I focus my attention on unhydrogenated samples. Then, by comparing the results with experiment observations, I speculate on the role of hydrogenation in determining the structure of  $\alpha$ -SiC. Previous theoretical work has been limited to the modeling of experimental results. Such a theoretical model, which has been recently employed in order to study the optical dielectric function of  $\alpha$ - $Si_{1-x}C_x$  alloys,<sup>51</sup> is the “tetrahedron model”<sup>52</sup> considering Si- and C-centered tetrahedra to be the fundamental structural units which determine the optical response of the films. This approach, though very useful for discussing the experimental results, is rather inadequate to account for the complex pattern of structural properties which these alloys seem to exhibit, and it can only be applied to the tetrahedral component of the material.

The present work (see also Ref. 31) is the first theoretical investigation of the liquid state of Si—C alloys. Our understanding of the liquid nature of semiconductor compounds is still in its infancy (even for the elemental systems) and it is not surprising that experimental results for this mixture are lacking. Nevertheless understanding of its properties could be important due to technological applications, such as crystal growth from the melt. Here, I predict some of these characteristics both at low and at high pressures. Of particular interest is the comparison of the amorphous and liquid states on the issue of chemical ordering and the strength of the Si—C bond. Also,

properties of pure  $l$ -C at high pressures will be discussed. This is related to the question of the slope of the diamond melting line in the phase diagram of carbon, which has lately attracted considerable attention.

## II. METHOD

The method used to study the properties of amorphous and liquid SiC is a type of direct simulation, free of experimental inputs and *a priori* assumptions about the network topology. Modeling the interatomic interactions in these disordered systems is a rather formidable task, given the variety of bonding possibilities ( $sp$  vs  $sp^2$  vs  $sp^3$ ) which might be displayed by carbon. A reliable description of the interatomic interactions and energetics is provided by using an empirical interatomic potential<sup>35</sup> which has been well tested in various applications. The severe mismatch of the two components (Si and C) and our intention to investigate disordered phases, where large bond-length and bond-angle distortions strongly influence the energetics of the system, require a stringent test of the potential. This is ensured by the reproduction<sup>35</sup> of properties of  $c$ -SiC in a variety of polytypes, and of properties of such disordered environments in the crystalline state as point defects (vacancies and interstitials).

Details about the development, functional form, and parameter values of the potential are given elsewhere.<sup>35</sup> Here, we mention that for the Si—Si and C—C interactions, the elemental empirical potentials for Si (Ref. 34) and C (Ref. 11), respectively, are used. These have been extensively tested (reasonable formation energies of defects, good elastic properties, etc.) and they have yielded accurate descriptions of the structural properties of  $\alpha$ -Si (Ref. 53) and  $\alpha$ -C (Refs. 11 and 15). Due to the crucial role that carbon plays in the disordered alloys it is important to note that the carbon potential describes well the variations of cohesive energies and bond lengths among carbon polytypes, especially for the lower-energy carbon structures graphite and diamond, and that it is able to distinguish between different carbon environments in disordered phases.

The liquid state of the elemental systems is also well described. In particular, the structural characteristics of  $l$ -C at low pressures<sup>47</sup> are in agreement with first-principles molecular-dynamics simulations<sup>27</sup> (both predict a coordination number for the liquid less than that of graphite). Liquid silicon, at the experimental liquid density, has a coordination number of  $\sim 5.8$  compared to a coordination number of  $\sim 6.4$  given by experiment.<sup>25</sup> However, the melting temperature of both Si and C is overestimated (the potentials are not fitted to the melting point), but this does not represent a serious problem since we are not interested in an accurate description of the melting line in the phase diagram.

The cross interactions Si—C are estimated using a simple extrapolation scheme from the elemental interactions, in which a single parameter multiplying the attractive term of the potential is chosen in such a way so that the cohesive energy of  $c$ -SiC (6.34 eV/atom) is reproduced (details in Ref. 35). The equilibrium lattice constant of  $c$ -SiC is 4.32 Å compared to the experimental value of

4.36 Å. Also, the elastic constants and the equilibrium bulk modulus are found to be in good agreement with experiment. This is particularly important when large distortions from equilibrium configurations are expected, as is the case here.

The present approach is necessarily less accurate than first-principles quantum-mechanical calculations. However, it has the advantage of great statistical precision (averages after extensive sampling in the configuration space), and allows the use of large cells to model the disordered geometry. In contrast, *ab initio* molecular-dynamics methods are so numerically intensive that they are restricted to short simulation times and small number of atoms.

In addition, the empirical potential approach offers the possibility of additional insight by extracting important quantities in disordered systems (as defect formation energies<sup>53</sup> and glass transition temperatures<sup>15,53</sup>), which are inaccessible by *ab initio* calculations. This is made possible by partitioning the total energy into atomic contributions.<sup>15,53</sup> Here, I follow a similar procedure by decomposing the total energy into bond energies, and studying in this way the strength of the Si—C bond in disordered environments.

A frequently made criticism of empirical potentials is that they neglect the interrelation between structural and electronic properties. One can compensate for that by performing quantum-mechanical calculations<sup>54</sup> on geometries which have been generated and extensively relaxed using reliable empirical potentials. In this manner one can selectively generate disordered local geometries (such as homopolar bonds, coordination defects, or atoms of different coordination) and study their effect on the band gap and the density of states of the material.

The formation of the disordered phases and the investigation of their properties is simulated using a continuous-space Monte Carlo (MC) algorithm.<sup>53</sup> Simulations are done with computational cubic cells of 216 atoms either by rapid quenching from the melt, or by homogeneously condensing the vapor. In the first procedure, which is usually used in simulations of amorphous materials, one begins with the crystal (the diamond or zinc-blended structure) at the equilibrium lattice constant. The sample is heated at constant temperature ( $\sim 5000$  K) and permitted to melt and equilibrate under small applied pressure ( $N, P, T$  ensemble). The melt is then cooled at inverse rates of  $\sim 10$ – $16$  MC steps/atom-K down to 300 K, where the pressure is removed and statistics are taken to obtain sample properties.

In the second procedure,<sup>11</sup> instead of starting from the dense liquid state, one begins from the dilute vapor phase. A huge cell is used, containing silicon and carbon atoms far apart from each other. The atoms must diffuse randomly for large distances before interacting and forming clusters, while at the same time the cell is allowed to slowly shrink under applied pressure (5–10 Kbars). The temperature at which this condensation is taking place is below the melting point, but high enough so that atoms can have the necessary mobility to avoid falling into a highly defective structure, where many atoms are undercoordinated or overcoordinated. After the volume equi-

brates the pressure is removed and the sample is gradually cooled to and equilibrated at 300 K. Both procedures described above lead to almost identical structures, demonstrating the existence of a well-defined amorphous geometry, independent of preparation conditions (i.e., conditions imposed on the computer simulation).

The liquid samples are generated by melting the crystal using a constant temperature and volume ( $N, V, T$ ) MC procedure. The fixed density is taken to be the average of the experimental liquid-silicon density,  $\rho = 2.59 \text{ gcm}^{-3}$  (Ref. 28), and a density for liquid carbon of  $\sim 2 \text{ gcm}^{-3}$  used in previous simulations,<sup>11,27</sup> because no experimental value for the density of *l*-SiC exists. As a test, calculations using the constant pressure-variable volume ( $N, P, T$ ) procedure, indicate that at the low- $P$  regime this is a reliable density for the liquid. The melting point of the compound is rather difficult to accurately estimate because of the short simulation times which are feasible. Therefore, the melt for stoichiometric samples is generated at 5000 K. The formation of a liquid structure is indicated by the rapid increase of the atomic mean-square displacement. When dealing with nonstoichiometric samples the temperature is fixed at various values depending on the carbon concentration.

### III. STRUCTURE

#### A. Amorphous silicon carbide

The most striking feature of the computer-generated models is that the amorphous network deviates from an ideal tetrahedral structure, since many of the carbon atoms are threefold coordinated. This, and much of other information about the network topology (specifically about short-range order) can be obtained by analyzing the radial distribution function  $g(r)$  of many samples. A typical  $g(r)$  for a stoichiometric sample, together with the partial functions, is shown in Fig. 1 and properties are summarized in Table I.

The prominent feature of the  $g(r)$  is the peak at 1.9 Å, arising from Si—C correlations, close to the first-neighbor bond length (1.86 Å with this potential) in the SiC crystal. The peak around 1.51 Å is due to correlations from first-neighbor carbon atoms. It is located between the graphite bond length (1.46 Å) and the diamond bond length (1.54 Å). The shoulder around 2.38 Å corresponds to first-neighbor Si—Si correlations (compared to 2.36 Å in *c*-Si). Second-neighbor Si—Si, C—C, and Si—C correlations merge to create the broad peak centered around 3.18 Å. Further information is obtained from the partial functions. It is seen that the second Si—Si peak is located at 3.18 Å, compared to 3.07 Å in *c*-SiC, while the second-neighbor peak of  $\alpha$ -Si at 3.84 Å is almost absent from this sample. Regarding C—C correlations, the second-neighbor interactions are split into two. One with a peak at 2.66 Å, where the two carbon atoms are bonded to another carbon atom (the corresponding distance in diamond is 2.52 Å), and the second with a peak at 3.20 Å, related to a configuration where the two carbon atoms are bonded to a silicon atom (the

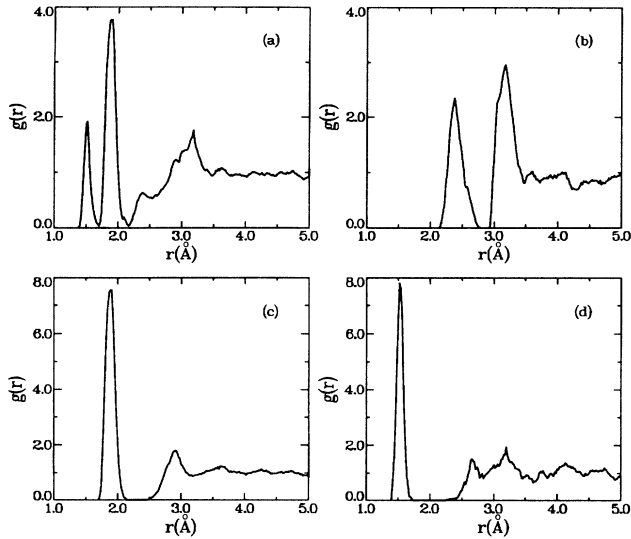


FIG. 1. Calculated radial distribution functions for stoichiometric amorphous silicon carbide (arbitrary normalization). (a) Total function. (b)–(d) are partial functions for Si—Si, Si—C, and C—C correlations, respectively.

corresponding distance of 3.07 Å is found in *c*-SiC). All of these bear significance on the question of chemical ordering (to be discussed in the next section). Here, we emphasize that both heteropolar and homopolar bonds exist in the amorphous network.

We define the nearest neighbors of a given atom as those falling within a distance less than that of the first dip in the radial distribution function. For a multicomponent system, such a distance must be separately defined for each type of atom pair. The partial coordinations are thus indicated by the areas under the first peaks (up to

the minimum) in the distribution functions, and are listed in Table I. We find that, on average, there are 1.75 silicon and 2.27 carbon atoms bonded to each silicon atom, i.e.,  $z_{\text{Si-Si}}=1.75$  and  $z_{\text{Si-C}}=2.27$ , while there are 1.19 carbon and 2.27 silicon atoms bonded to each carbon atom, i.e.,  $z_{\text{C-C}}=1.19$  and  $z_{\text{C-Si}}=2.27$ . In total, silicon has 4.02 nearest neighbors,  $z_{\text{Si}}=4.02$ , and carbon has 3.46 nearest neighbors,  $z_{\text{C}}=3.46$ . The amorphous structure, therefore, can not be described as a tetrahedral network since about half the carbon atoms are threefold coordinated.

Such threefold local geometries cannot be viewed as defects (unsaturated, dangling bonds) in a tetrahedral network but they are truly graphitelike. This is nicely depicted in the bond-angle distributions of carbon atoms (i.e., having a carbon atom as the vertex atom), which are shown in Fig. 2. The distinction between threefold and fourfold distributions is clear. The former is peaked around the graphite bond angle of 120°, while the latter is peaked at about the tetrahedral bond angle of 109°. It is also evident from the width of the two distributions that the  $sp^3$  sites are rather more distorted than the  $sp^2$  configurations. A similar conclusion, regarding  $sp^3$  sites in amorphous carbon ( $\alpha$ -C), has been reached by Galli *et al.*,<sup>12</sup> from structural observations, and by the author, based on energetics arguments ( $sp^3$  geometries have higher atomic energies than  $sp^2$  sites).<sup>15</sup>

The distinction between  $sp^2$  and  $sp^3$  sites can be further enhanced considering the bond lengths in the sample. It is found that, on the average, a threefold carbon atom has a nearest-neighbor carbon atom located at a distance of 1.48 Å. In the case, where the two carbon atoms are both threefold coordinated, their bond length approaches the graphitic value (1.46 Å). For  $sp^3$  atoms, the  $C_4$ —C bond length is equal to 1.54 Å, while the  $C_4$ — $C_4$  bond lengths are somewhat larger ( $\sim 1.56$  Å) than the diamond value. The distribution of the graphitic and diamondlike bonds in the network is almost random. Regarding the coordi-

TABLE I. Calculated properties of a stoichiometric amorphous sample at 300 K; positions of peaks (in Å) in the radial distribution functions for various correlations, average partial coordinations  $z$ , and “random” coordinations  $z^R$  (as explained in the text). Numbers in parentheses give equivalent distances in respective crystals.

Correlations	$r_1$	$r_2$	$r_3$	$z$	$z^R$
C—Si	1.90 (1.88) <sup>a</sup>	2.92	3.62 (3.60) <sup>a</sup>	2.27	1.86
Si—Si	2.38 (2.36) <sup>b</sup>	3.18 (3.07) <sup>a</sup>	(3.84) <sup>b</sup>	1.75	2.16
C—C	1.51 (1.46) <sup>c</sup>	2.66 (2.52) <sup>d</sup>	3.20 (3.07) <sup>a</sup>	1.19	1.60
	(1.54) <sup>d</sup>				
$C_3$ — $C^{(e)}$	1.48	2.69	3.25	1.41	1.50
$C_3$ — $C_3$	1.46	2.67	3.22	0.78	
$C_3$ — $C_4$	1.50	2.71	3.28	0.63	
$C_4$ —C	1.54	2.64	3.16	0.93	2.00
$C_4$ — $C_4$	1.56	2.60	3.14	0.41	
$C_4$ — $C_3$	1.50	2.71	3.28	0.52	

<sup>a</sup>In *c*-SiC.

<sup>b</sup>In *c*-Si.

<sup>c</sup>In graphite.

<sup>d</sup>In diamond.

<sup>e</sup> $C_3, C_4$  denote threefold- and fourfold-coordinated carbon atoms, respectively.

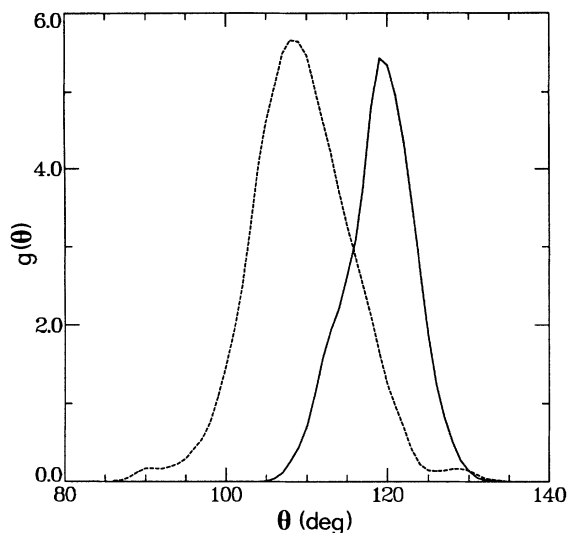


FIG. 2. Bond-angle distributions for carbon atoms (arbitrary normalization). Solid line, threefold; dashed, fourfold.

nation of silicon, the slight deviation from an average number of four is attributed to the presence of defects, most of them fivefold coordinated atoms.<sup>8,53</sup> The number of these defects can be reduced by extended annealing during or after condensation.

Analyzing in this way many samples, it is found that homopolar bonds always exist, and that the number of  $sp^2$  graphitelike sites ranges from  $\sim 40\%$  to  $\sim 65\%$ . Larger applied pressure during condensation tends to promote in some degree  $sp^3$  carbon bonding (reaching  $\sim 75\%$ ) as it was also observed in simulations of  $\alpha$ -C.<sup>11,15</sup> However, from some values of pressure and above, the increase in fourfold carbon bonding is accompanied by significant overcoordination of silicon, something unacceptable. Subsequent annealing of such a high-pressure phase then results to the elimination of silicon overcoordination, but at the same time the number of  $sp^3$  carbon sites is also reduced, so that a perfectly tetrahedral structure could never be achieved.

The density of the stoichiometric samples range from 75% to 81% of the density of  $c$ -SiC, as it can be seen from Table II, and it increases with fourfold carbon coordination. For comparison we note that  $\alpha$ -Si is less dense than  $c$ -Si by 1–10%. Thus, the somewhat smaller density ratio among  $\alpha$ -SiC and  $c$ -SiC is attributed to the gra-

TABLE II. Calculated volume per atom  $\Omega_{at}$ , corresponding number density  $\rho_N$ , and excess density  $\Delta\rho_N$  for  $\alpha$ -SiC and other relevant structures.

	$\Omega_{at}(\text{\AA}^{-3})$	$\rho_N(\text{\AA}^{-3})$	$\Delta\rho_N(\text{\AA}^{-3})$
$c$ -Si	20.0	0.05	
$c$ -C (diamond)	5.64	0.177	
ZB $c$ -SiC	10.08	0.099	-0.015
$\alpha$ -Si	$\sim 20.57$	0.049	
$\alpha$ -C (diamondlike)	$\sim 6.33$	0.158	
$\alpha$ -C (evaporated)	$\sim 9.94$	0.100	
$\alpha$ -SiC	$\sim 12.57$	0.074–0.082	$\sim 0.02 - \sim 0.0$

phitically bonded carbon atoms, favoring a more open structure. Recall that the density of evaporated  $\alpha$ -C is only  $\sim 55\%$  of the density of diamond.<sup>9–12,15</sup> If we define the excess macroscopic density  $\Delta\rho_{AB} = \rho_{AB} - \frac{1}{2}(\rho_A + \rho_B)$ , measuring the deviation of the density in the heteropolar system from the average value in its homopolar constituents, we see that  $\Delta\rho_{c-SiC}$  is negative, which simply reflects that  $c$ -SiC shows a negative deviation from Vegard's rule ( $\Delta\alpha_{SiC} = -0.17 \text{ \AA}$ ). A similar quantity could be defined for  $\alpha$ -SiC, where now the homopolar constituents would be  $\alpha$ -Si and  $\alpha$ -C. This gives a negative  $\Delta\rho_{\alpha-SiC}$  only if we choose for  $\rho_{\alpha-C}$  diamondlike densities. If evaporated  $\alpha$ -C densities are taken then  $\Delta\rho_{\alpha-SiC}$  is about zero.

Direct, experimental evidence for homopolar bonds in  $\alpha$ -SiC is provided by Gorman and Solin,<sup>46</sup> who used Raman spectroscopy to analyze carbon-deficient ( $\alpha$ -Si<sub>0.59</sub>C<sub>0.41</sub>) sputtered films. They have clearly observed both graphitelike and diamondlike C—C bonds, which are less likely to occur in a silicon-rich sample. They emphasize, however, that the coordination remains fourfold. This means that even in the case of graphitelike bonding, the relevant geometry is a distorted tetrahedron, where a central carbon atom is bonded to other carbon atoms (bondlengths of  $\sim 1.46 \text{ \AA}$ ), but also to silicon atoms. Bond angles then, are not graphitelike ( $\sim 120^\circ$ ) but rather distorted tetrahedral. Here, without excluding the above possibility, we find that tetrahedra with carbon at the center mostly contain diamondlike bonds ( $\sim 1.50$ – $1.56 \text{ \AA}$ ). Shorter, graphitelike bonds ( $\sim 1.46 \text{ \AA}$ ) are rather associated with threefold arrangements. It should be mentioned however, that the observation of homopolar bonds in  $\alpha$ -SiC by Gorman and Solin is disputed by other experiments. In particular, infrared-absorption measurements in sputtered films by Fagen<sup>49</sup> have been interpreted as indicating a very small number of homonuclear bonds. The same conclusion is reached by Kaloyeros, Rizk, and Woodhouse<sup>45</sup> from EXAFS and EXELFS measurements on sputtered films too.

Unavoidably related to the issue of homopolar bonding is the question of carbon coordination. As it is mentioned above, the mere existence of graphitelike ( $\sim 1.46 \text{ \AA}$ ) C—C bonds in the samples is associated with threefold carbon coordination. The present results however, should be viewed as a qualitative description of the amorphous structure, rather than an accurate estimation of the number of  $sp^2$  graphitelike sites. Therefore, a quantitative comparison with experimental results is rather difficult, more so when taking into account that there is evidence<sup>44</sup> that carbon coordination is affected by different preparation conditions. Obviously, the computer simulations do not recreate the fine details and the actual kinetics, during deposition, of each distinct preparation method but they generate a well-defined amorphous structure where general trends can be observed. In any case, the present suggestion for  $sp^2$  carbon bonding in  $\alpha$ -SiC is supported by recent *ab initio* molecular-dynamics simulations,<sup>55</sup> and by EXAFS and x-ray-scattering studies.<sup>56</sup> Also, the existence of threefold-coordinated carbon in evaporated  $\alpha$ -SiC is directly indicated by the presence of a strong  $\pi^*$  peak in the EELS spectra of McKenzie, Berger, and Brown.<sup>47</sup> It is surprising, however, to see

that electron-diffraction results in the same material are interpreted as indicating a predominantly tetrahedral network.<sup>50</sup> A similar description is given by the EXAFS and EXELFS measurements of Kaloyeros, Rizk and Woodhouse.<sup>45</sup>

Further insight to the issue of carbon coordination can be derived by looking at nonstoichiometric samples. Increasing the carbon concentration in the samples, unquestionably results in an increase of  $sp^2$  sites, reaching 85–90% for  $x_C=1.0$ , i.e., for  $\alpha$ -C. The reason for this trend is obvious. With less silicon atoms in the sample, the probability for a given carbon atom to be bonded graphitically to other carbon atoms in its neighborhood, under conditions of low pressure, is significantly increased. On the other hand, by moving to the opposite direction of increasing silicon content, the probability for a carbon atom to find other carbon atoms as nearest neighbors becomes smaller, and as a result one finds a trend for increasing  $sp^3$  site concentration.

A close look at both stoichiometric and nonstoichiometric samples shows no evidence for phase separation into a Si-rich or C-rich region, i.e., the samples are homogeneous. This is in agreement with the experimental observations of Gorman and Solin,<sup>46</sup> who argue that phase separation of C into an amorphous carbon region is excluded because the optical-absorption edge of their films shifts toward the blue upon annealing at 600°C, while the absorption edge of  $\alpha$ -C shifts toward the red. A somewhat more sensitive issue to tackle is whether there is any clustering of carbon  $sp^3$  sites, as it has been observed in simulations of  $\alpha$ -C by Galli *et al.*<sup>12</sup> From the stoichiometric sample of Table I we estimate the ratio  $z_{44}/z_{43} \approx 0.79$ , by counting the neighbors from the  $g_{44}(r)$  and  $g_{43}(r)$  partial distributions functions, and compare it with the value  $N_4/N_3=0.83$  ( $N_4=49$  and  $N_3=59$  is the number of  $sp^3$  and  $sp^2$  sites, respectively), which is obtained from a random distribution of  $sp^3$  atoms. Thus, contrary to  $\alpha$ -C, no clustering is observed. However, by going to nonstoichiometric, carbon-rich samples, some small degree of clustering appears and gets bigger when approaching  $x_C=1.0$  (not as large as in Ref. 12, though). We therefore conclude that the presence of silicon prevents the clustering of  $sp^3$  sites.

Having dealt in detail with the question of coordination, we now speculate about the effect of hydrogenation. It is worth recalling that measurements<sup>9,10</sup> in evaporated amorphous carbon, confirmed by theoretical calculations,<sup>11,12</sup> indicate small  $sp^3$  site concentrations (1–20%). However, hydrogenated amorphous carbon ( $\alpha$ -C:H) contains far more  $sp^3$  sites ( $\sim 70\%$ ).<sup>9</sup> This suggests the possibility that hydrogenation might also promote fourfold coordination in  $\alpha$ -SiC. EELS spectra<sup>48</sup> of silicon-rich  $\alpha$ -SiC:H indicate fourfold-coordinated C atoms, though it is believed<sup>51</sup> that carbon-rich specimens still contain a considerable amount of  $sp^2$  carbon atoms. Note that for these carbon-rich samples, incorporation of hydrogen in large amounts results, as in the case of  $\alpha$ -C, not only in an enhancement of some diamondlike properties (fourfold coordination and large optical gaps), but also to the development of soft polymeric regions, which are responsible for deteriorating the hardness of the ma-

terial.

To close the discussion about the structure of  $\alpha$ -SiC, we make a direct comparison of the present, theoretical structural model with available experimental results on the basis of a structure factor analysis. Figure 3(a) shows the computed total structure factor  $S(k)$  for a nonstoichiometric sample ( $\alpha$ -Si<sub>0.75</sub>C<sub>0.25</sub>). Positions of intensity maxima from electron-diffraction results,<sup>48</sup> from a sample of about the same composition ( $\alpha$ -Si<sub>0.68</sub>C<sub>0.32</sub>), are also shown for comparison [the actual shape of the experimental  $S(k)$  is not given]. The agreement is excellent, even for low  $k$  values, indicating the close relation of the computer-generated network with the real material. The dominant peak in the structure factor is at  $3.86 \text{ \AA}^{-1}$  (compared with the pronounced experimental maximum at  $3.90 \text{ \AA}^{-1}$ ), and arises from both nearest- and next-nearest-neighbor contributions, mainly from Si—C bonds, as can be seen from the partial structure factors shown in Figs. 3(b)–3(d). The inner peak of  $2.12 \text{ \AA}^{-1}$  arises from second-nearest neighbors, mainly from C—C interactions, while only first-neighbor correlations are believed to contribute for  $k > 5 \text{ \AA}^{-1}$ . Note that the experimental sample is hydrogenated, but this does not alter the conclusions of the comparison. The reason is that the presence of hydrogen is not expected to directly have significant effects on  $S(k)$  because of the small scattering power of hydrogen. It could indirectly make some changes through the atoms bonded to it though.

### B. Liquid silicon-carbon alloys

Bonding in liquid mixtures of silicon and carbon is even more complex than in the amorphous counterpart. This is due to the wide variety of coordinations that both

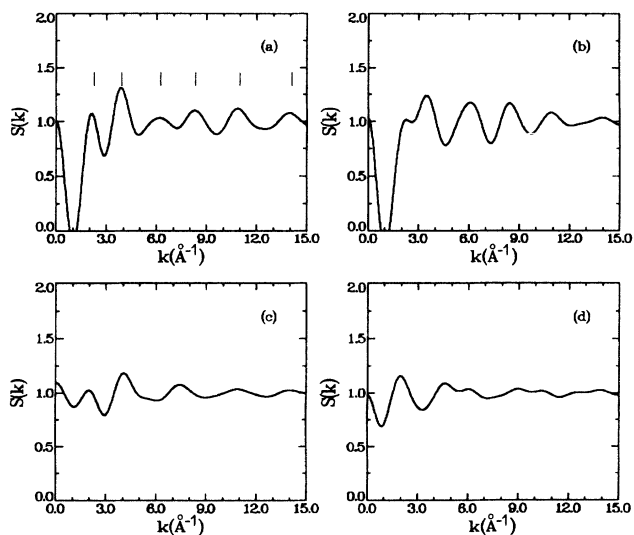


FIG. 3. Calculated structure factors for a nonstoichiometric sample ( $\alpha$ -Si<sub>0.75</sub>C<sub>0.25</sub>). (a) Total function. Vertical bars indicate positions of intensity maxima from electron diffraction results for a Si<sub>0.68</sub>C<sub>0.32</sub> sample (Ref. 9). (b)–(d) are partial functions for Si—Si, Si—C, and C—C correlations, respectively.



elements can exhibit in the liquid state, and because there is an intriguing competition among them in imposing their own favorable liquid structure. In fact, the most interesting finding of the simulations is that silicon behaves quite differently in the liquid alloys, at low pressures, compared to the amorphous ones. In the latter, silicon keeps the fourfold coordination that it has in the homopolymers, e.g.,  $\alpha$ -Si. In the former, it is "forced" by carbon to assume a coordination much lower than in  $l$ -Si, enhancing in this way the covalent bonding which persists in  $l$ -SiC. Things do change, however, at high pressures.

We first begin by discussing properties of the liquid at low pressures. Figure 4 shows the radial distribution function  $g(r)$  for a stoichiometric sample, along with the partial functions. Calculated properties are summarized in Table III. Although the peaks of the total function are considerably widened and flattened, compared to the  $g(r)$  of the amorphous phase, we can identify three distinct features. There is a shoulder at  $\sim 1.5$  Å arising from first-neighbor C—C correlations, a peak at  $\sim 1.9$  Å arising from first-neighbor Si—C correlations, and the next very broad peak containing first-neighbor Si—Si correlations as well as second-neighbor Si—Si, Si—C, and C—C correlations. The contribution to the total  $g(r)$  from each type of correlation becomes evident by analyzing the partial functions. It is seen that the average first-neighbor Si—Si distance is  $\sim 2.52$  Å, close to the respective distance of 2.5 Å in  $l$ -Si,<sup>25</sup> while the second-neighbor distance is peaked at  $\sim 3.3$  Å, compared to 3.78 Å in  $l$ -Si. The average Si—C bond length is 1.92 Å, slightly larger than the respective crystalline value of 1.88 Å. This is also true for the second-neighbor distance. On the other hand, the first-neighbor C—C distance slightly decreases (1.48 Å), while the second-neighbor distance becomes

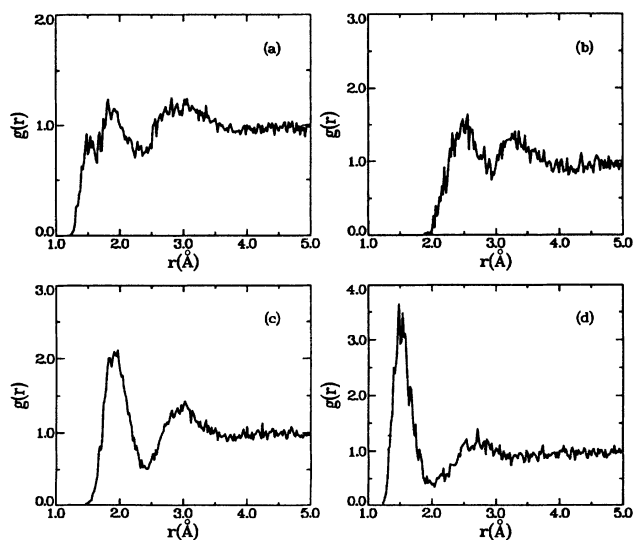


FIG. 4. Calculated radial distribution functions for stoichiometric liquid silicon-carbon alloy (arbitrary normalization). (a) Total function. (b)–(d) are partial functions for Si—Si, Si—C, and C—C correlations, respectively.

TABLE III. Calculated properties of a 50%-50% liquid sample at  $T=5000$  K; positions of peaks (in Å) in the  $g(r)$  for various correlations, average partial coordinations  $z$ , and "random" coordinations  $z^R$  (as explained in the text).

Correlations	$r_1$	$r_2$	$z$	$z^R$
Si—Si	2.52	3.30	2.94	2.89
Si—C	1.92	3.02	1.85	1.90
C—C	1.48	2.70	1.29	1.24
Si <sub>4</sub> —Si	2.40	3.10	2.30	
Si <sub>5</sub> —Si	2.46	3.26	3.20	
Si <sub>6</sub> —Si	2.64	3.36	3.50	
C <sub>2</sub> —C	1.40	2.52	0.9	
C <sub>3</sub> —C	1.46	2.69	1.25	
C <sub>4</sub> —C	1.54	2.72	1.60	

larger (2.70 Å), compared to the respective distances in the amorphous samples. A similar behavior was also observed in previous simulations of  $l$ -C.<sup>27</sup>

Figure 5 shows the calculated structure factors (total and partial) for the stoichiometric sample of Table III. No experimental results exist for comparison. The dominant peak in the total  $S(k)$  is at  $\sim 4.5$  Å<sup>-1</sup> and seems to be arising mainly from Si—C correlations and from some C—C contributions as well. The inner peak at  $2.6$  Å<sup>-1</sup>, on the other hand, originates from Si—Si correlations. These have a similar overall behavior as in the elemental system,<sup>25</sup> but here the height of the peaks is smaller and their position is a bit moved toward lower  $k$  values. We can also make a comparison between the  $S(k)$  for C—C interactions in the liquid alloy, Fig. 5(d), and the  $S(k)$  of elementary  $l$ -C ( $\rho \sim 2$  g cm<sup>-3</sup>) shown in Fig. 6(a). We ob-

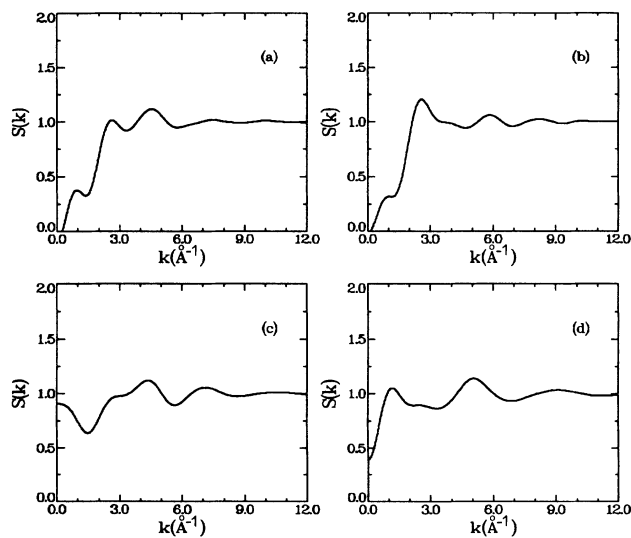


FIG. 5. Structure factors for the stoichiometric sample of Fig. 4. (a) Total function. (b)–(d) are partial functions for Si—Si, Si—C, and C—C correlations, respectively.



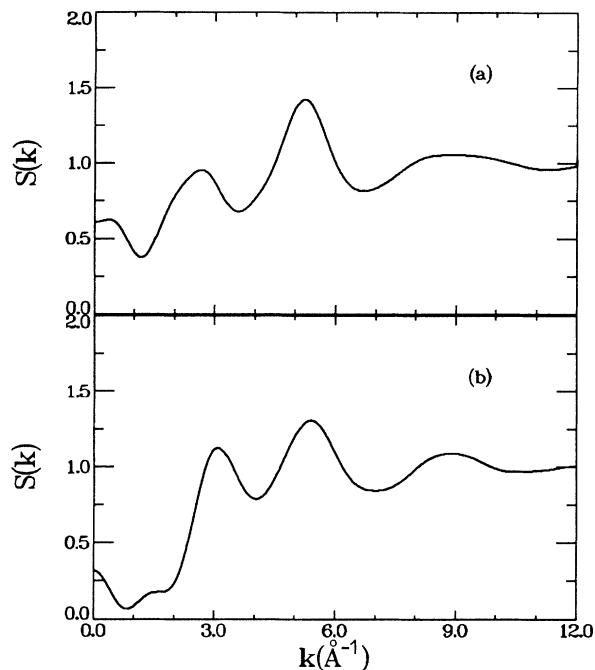


FIG. 6. (a)  $S(k)$  of elemental liquid carbon (7000 K). (b)  $S(k)$  of  $l$ -C at 1-Mbar pressure and 9000 K.

serve a drastic decrease of the height of the dominant peak at  $\sim 5.1 \text{ \AA}^{-1}$ , while the inner peak at  $\sim 2.7 \text{ \AA}^{-1}$  is being replaced by a weak shoulder. Interestingly, another peak at low  $k$  values ( $\sim 1.2 \text{ \AA}^{-1}$ ) appears. It would be nice if experimental structure factors could become available in order to check these predictions.

The average partial coordinations, which are listed in Table III, can be estimated by integrating the partial distribution functions up to the first minimum. We find that the majority of carbon atoms in the liquid are threefold coordinated ( $\sim 66\%$ ). About 24% are fourfold and the remaining twofold coordinated. As seen from Table III, C—C bonds become shorter with decreasing coordination. In the case of twofold sites, the average  $C_2$ —C distance is  $\sim 1.4 \text{ \AA}$ , but when bonded to each other the  $C_2$ — $C_2$  bond is even shorter ( $\sim 1.37 \text{ \AA}$ ). Such values indicate triple bonds among carbon atoms. However, as in the liquid the bonds are continuously being formed and broken, the average number of such triple bonds is small, and twofold sites are mostly connected to threefold carbon sites as well as to fourfold and fivefold silicon sites.

Additional information about carbon atoms in the liquid is obtained from their bond-angle distribution functions, shown in Fig. 7(a). The distribution between threefold- and fourfold-coordinated atoms is clear since the former have a distribution with a maximum at about the graphite bond angle of  $120^\circ$ , while the latter's distribution has a maximum at the tetrahedral bond angle of  $109^\circ$ . Both distributions are quite broad, much broader than the respective distributions in the amorphous alloys (Fig. 2), indicating significant distortion of  $sp^2$  and  $sp^3$  units. Twofold-coordinated atoms have a wide range of preferred bond angles, mostly larger than  $100^\circ$ .

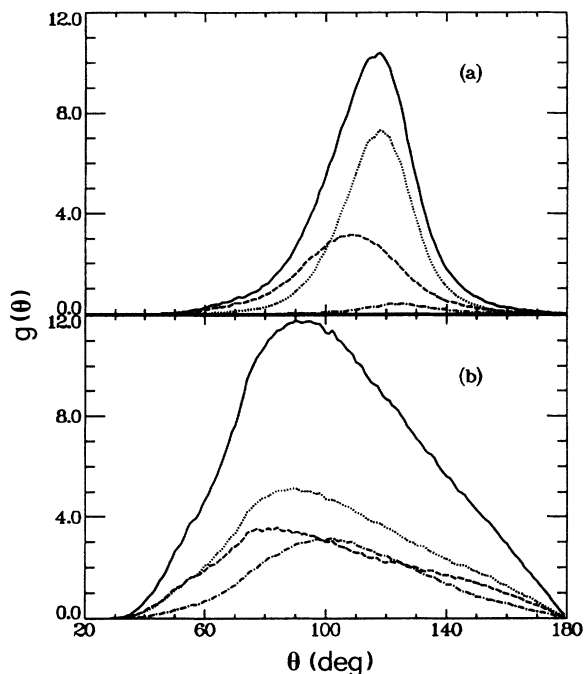


FIG. 7. Bond-angle distributions (arbitrary normalization). (a) For carbon atoms: solid line, total; dashed, fourfold; dotted, threefold; dashed-dotted, twofold. (b) For silicon atoms: solid line, total; dashed, sixfold; dotted, fivefold; dashed-dotted fourfold.

Regarding silicon atoms, we find that about 38% are fourfold, 44% are fivefold, and the rest sixfold coordinated. As expected, Si—Si bond lengths are larger when involving atoms of higher coordinations. On the other hand, increasing coordination leads to lower values for the bond angles (having Si atoms as vertex atoms), as shown in Fig. 7(b). The total bond-angle distribution is unimodal with a maximum at about  $90^\circ$ . In contrast, Stich, Car, and Parrinello<sup>57</sup> find a bimodal distribution (with maxima at  $\sim 60^\circ$  and  $\sim 90^\circ$ ) in simulations of  $l$ -Si.

From the partial coordinations in Table III, we estimate the average total coordination of silicon in the stoichiometric liquid to be  $\sim 4.8$ ,  $z_{Si} \approx 4.8$ . This is in marked contrast to the silicon coordination number in  $l$ -Si, which is  $\sim 5.8$ – $6.0$  with this potential. Similarly, a high coordination number of Si ( $\sim 6.0$ ) exists in  $l$ -SiGe alloys (as simulations using the potential of Ref. 35 show). Therefore, the strong reduction should be correlated to the low coordination number of carbon, which has on average  $\sim 3.1$  nearest neighbors,  $z_C \approx 3.1$ . Comparing this number with the coordination in  $l$ -C of  $\sim 2.8$ – $2.9$ , we observe an increase in carbon coordination in the alloy but not as drastic as the reduction in silicon coordination. Thus, it seems that carbon retains a low  $z_C$  and imposes, as a result, a rather open structure. We recall that the coordination in  $l$ -Si is already low compared to the coordination in most liquid metals ( $\sim 12$ ), indicating a persistence of covalent bonds in the liquid.<sup>25,32,57</sup> Here, we find that the presence of carbon induces an even larger tendency toward local tetrahedral

order and covalent bonding. Such covalent bonds must form between atoms separated by a distance less than a maximum length. Stich, Car, and Parrinello<sup>57</sup> find this cutoff distance  $r_c$  in *l*-Si to be  $\sim 2.49$  Å. I similarly find a covalent distance of 2.40 Å for Si<sub>4</sub>—Si bonds and 2.46 Å for Si<sub>5</sub>—Si bonds. “Metallic” bond lengths are exhibited by sixfold atoms. Also, we observe that the number of fourfold Si atoms is considerably increased in the alloy compared to the respective number in *l*-Si.

To appreciate more the above behavior, it is worth to get an overview of it with carbon composition. Figure 8 shows the resulting variation in the total coordinations of Si and C. Although both have a linear dependence on  $x_C$ , the effect is more crucial for Si. We observe that its coordination approaches the value it has in *l*-Si, with decreasing carbon content, but it falls off quite rapidly and approaches the value of 4.0 in the carbon-rich liquid. On the other hand, the variation of  $z_C$  is much less steep than for Si. It slowly increases with silicon content and retains low value even in the carbon-deficient samples. We therefore conclude that carbon mainly prefers graphitelike  $sp^2$  bonding in these liquid alloys. For carbon concentration  $x_C > 0.5$ ,  $sp$  bonding becomes important too, while for  $x_C < 0.5$ , the liquid contains a considerable number of distorted  $sp^3$  units.

Having analyzed in detail the properties of the liquid at low pressures, we now wish to study the structure at higher pressures. For this end we follow a different approach. Instead of fixing the density of the liquid (somewhat arbitrarily) at a given temperature and then *a posteriori* estimating the pressure, as done in previous simulations of *l*-C at high  $P$ ,<sup>58</sup> we allow density and volume fluctuations using the isothermal-isobaric ensemble ( $N, P, T$ ) which precisely fixes temperature and pressure. With this procedure, a number of samples is generated by fixing the pressure and equilibrating the liquid at the appropriate temperature.

The results are summarized in Fig. 9, showing the variations in total coordinations with increasing pressure, for

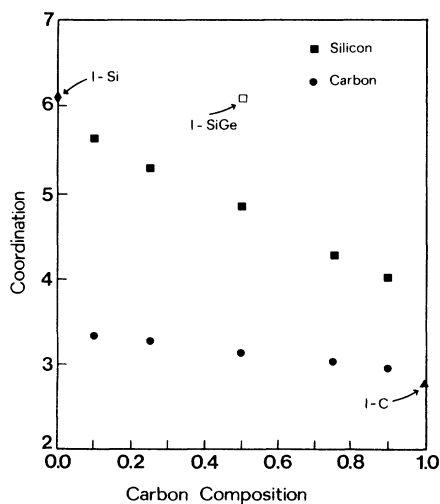


FIG. 8. Coordinations vs carbon composition. Respective number for 50%-50% *l*-SiGe is also shown for comparison.

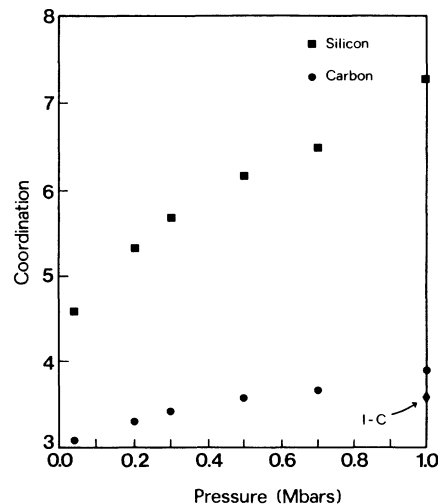


FIG. 9. Coordinations vs pressure, for a stoichiometric sample. Also shown is coordination of *l*-C at 1-Mbar pressure.

a 50%-50% sample. Again, there is remarkable difference in the behavior of the two elements. Silicon coordination rapidly increases with pressure, resulting from the gradual disappearance of fourfold atoms in favor of higher coordinations. Carbon coordination, however, is kept at low values and does not exceed four nearest neighbors even at the highest pressure considered (1 Mbar). This has its effect on the density of *l*-SiC, which is less dense than ZB *c*-SiC up to the pressure of  $\sim 600$  kbars. At 1-Mbar pressure the liquid is only  $\sim 8\%$  denser than the crystal. At this high- $P$  regime, fourfold carbon atoms are predominant, while threefold atoms are less numerous and twofold atoms are absent. Some fivefold atoms appear, but they are usually associated with a weak bond, having length close to the minimum in the  $g(r)$ , due to thermal fluctuations. In other words, we should not consider fivefold coordination as a natural bonding configuration of carbon even in the high- $P$  liquid.

Of great interest are also the properties of pure *l*-C at high  $P$ . This subject has attracted much attention in recent years. The present simulations show, see Fig. 9, that *l*-C is less dense than diamond even at 1-Mbar pressure and  $T=9000$  K. The structure factor of the high- $P$  liquid is shown in Fig. 6(b). Carbon has an average coordination of  $\sim 3.7$ , slightly less than in the Si—C system. Observations at neighboring pressures and temperatures lead to the same conclusions. Although these simulations are far from tracing the whole region near the melting line, they might indicate a positive slope of the diamond melting line in the phase diagram of carbon. However, more precise studies of the diamond-liquid carbon phase boundary will be needed in the future. The possibility that *l*-C is less dense than diamond<sup>59</sup> has significant implications in the fields of geology and astronomy, and it has been supported by various experiments<sup>60–62</sup> and by *ab initio* molecular-dynamics simulations.<sup>58</sup> The present results give further support to such high- $P$  properties of *l*-C.

#### IV. ENERGETICS—ORDERING

The question of chemical ordering, that is the predominance or not of heteropolar bonding, is a crucial issue to be tackled in the study of these alloys. We have already seen that homopolar bonds are an important ingredient in the description of the amorphous phase, and they are unquestionably present in the liquid. We would now like to make a more quantitative estimate of the ordering and explain its existence or not in energetics arguments.

Let us first count heteropolar bonds in the samples. If the atoms were to be distributed completely randomly, then the "random" coordinations in stoichiometric samples would be

$$\begin{aligned} z_{\text{Si-Si}}^R &= z_{\text{Si}} \times z_{\text{Si}} / (z_{\text{Si}} + z_{\text{C}}), \\ z_{\text{Si-C}}^R &= z_{\text{Si}} \times z_{\text{C}} / (z_{\text{Si}} + z_{\text{C}}), \\ z_{\text{C-C}}^R &= z_{\text{C}} \times z_{\text{C}} / (z_{\text{Si}} + z_{\text{C}}), \end{aligned} \quad (1)$$

where  $z_{\text{Si}}, z_{\text{C}}$  are the average coordination of silicon and carbon, respectively. Random coordinations  $z^R$  are listed in Table I for a stoichiometric, amorphous sample and in Table III for a stoichiometric, liquid sample. A measure of heteropolar bonding, and hence the degree of chemical order, is provided by the comparison of  $z_{\text{C-Si}}$ , the average number of heteropolar bonds, with the number for the case of zero chemical order,  $z_{\text{Si-C}}^R$ .

This yields a significant degree of ordering in the amorphous sample ( $z_{\text{C-Si}} = 2.27$  vs  $z_{\text{Si-C}}^R = 1.86$ ), although still far from the maximum possible ordering, which would be  $z_{\text{C-Si}} = 3.46$ . Of course, a clear indication of the partial ordering is provided by the dominant Si—C peak in the  $g(r)$  in Fig. 1(a). Besides that, ordering is indicated by the strong second Si—Si peak at 3.18 Å, shown in Fig. 1(b), and by the second-neighbor C—C peak at 3.20 Å (here the two carbon atoms are bonded to a silicon atom), shown in Fig. 1(d). The C—C peak at 2.66 Å, which indicates homopolar bonds (the carbon atoms are bonded to another carbon atom), is less pronounced.

Contrary to the observations in the amorphous sample, we find that the liquid is characterized by zero ordering, the distribution of atoms is random ( $z_{\text{Si-C}} = 1.85$ ,  $z_{\text{Si-Si}}^R = 1.90$ ). The small difference between  $z_{\text{Si-C}}$  and  $z_{\text{Si-Si}}^R$  is within the uncertainties when extracting the number of first nearest neighbors from the  $g(r)$ . Let us recall the ZB *c*-SiC has a large negative enthalpy of formation,  $\Delta H = -0.34$  eV/atom,<sup>18</sup> which entirely favors heteropolar bonds. Therefore we observe a gradual decrease of chemical ordering, from the solid (complete), to the amorphous (partial), to the liquid (zero). This can be attributed to the weakening of the Si—C bond due to high- $T$  fluctuations and maximization of disorder in its local environment.

In order to further examine this weakening, we study the energetics of the system by decomposing its total energy  $E$  into bond energies  $V_{ij}$ ,

$$E = \frac{1}{2} \sum_{i \neq j} V_{ij}, \quad (2)$$

where the indices  $i$  and  $j$  run over the atoms of the sys-

tem. Such a partitioning of the cohesive energy of the sample is explicitly specified in the definition of the interatomic potential used here.<sup>35</sup> A similar partitioning of the cohesive energy into site energies  $E_i$  has already given valuable information on the atomic-scale behavior of disordered systems, such as properties of defects in  $\alpha$ -Si,<sup>53</sup> stability of diamondlike  $\alpha$ -C,<sup>15</sup> and segregation in semiconductor-alloy surfaces.<sup>22</sup>

The results of this analysis for the stoichiometric amorphous sample are portrayed in Fig. 10(a), which shows the distributions of bond energies for each type of atom pair.  $P(E)$  is the probability of finding a bond at energy  $E$ . Note that in this scheme,  $V_{ij}$  depends on its local environment (type of neighboring bonds, coordinations of atoms  $i$  and  $j$ , etc.), and it is not just a pair-type interaction. Thus, in principle, the strength of the Si—C bond in the disordered phase may significantly deviate from its value in ordered, tetrahedral ZB *c*-SiC. Then, after extracting the average bond energies  $V_{\text{Si-Si}} \approx -2.0$  eV,  $V_{\text{C-C}} \approx -4.87$  eV, and  $V_{\text{Si-C}} \approx -3.52$  eV, we can get a measure of the tendency toward ordering, by considering

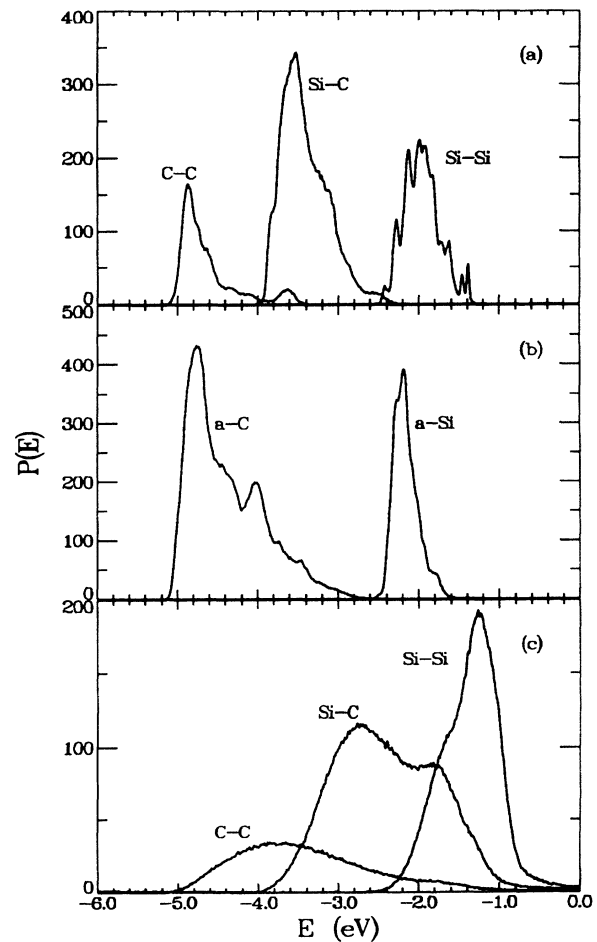


FIG. 10. Distributions  $P(E)$  of bond energies. (a)  $P(E)$  for a stoichiometric amorphous sample. (b)  $P(E)$  for the elemental systems  $\alpha$ -Si and  $\alpha$ -C. (c)  $P(E)$  for a stoichiometric liquid sample.

the excess bond energy  $\Delta V_{\text{Si-C}}$ ,

$$\Delta V_{\text{Si-C}} = V_{\text{Si-C}} - \frac{1}{2}[V_{\text{Si-Si}} + V_{\text{C-C}}]. \quad (3)$$

We find that  $\Delta V_{\text{Si-C}} \simeq -0.09$  eV (or  $\sim -0.18$  eV/atom, compared to  $-0.34$  eV/atom in *c*-SiC), which means that the SiC bond is still stabler than the average of Si—Si and C—C bonds, and it therefore drives the system into partial ordering.

It is not clear, however, if the reference level, against which the strength of the Si—C bond in the alloy is compared, should be derived from the same sample. Alternatively, we could take  $V_{\text{Si-Si}}$  and  $V_{\text{C-C}}$  as the average bond energies in the homopolar constituents  $\alpha$ -Si ( $\sim -2.2$  eV) and  $\alpha$ -C ( $\sim -4.70$  eV), shown in Fig. 10(b), which would then give  $\Delta V_{\text{Si-C}} \simeq -0.07$  eV, in agreement with the first choice.

If one is not interested in these details about the Si—C bond, information about the stability of the disordered phase can be obtained by just looking at the total energies. Then, we could define an “enthalpy of formation” of the amorphous phase  $\Delta H(\alpha\text{-SiC})$  with respect to the enthalpies of  $\alpha$ -Si and  $\alpha$ -C phases,

$$\Delta H(\alpha\text{-SiC}) = H(\alpha\text{-SiC}) - \frac{1}{2}[H(\alpha\text{-Si}) + H(\alpha\text{-C})]. \quad (4)$$

Average total energies are listed in Table IV (among other properties). Then Eq. (4) gives an enthalpy of formation of  $\sim -0.10$  eV/atom, again in reasonable agreement with the results obtained by decomposing the energy. That  $\Delta H(\alpha\text{-SiC})$  is negative means that the amorphous alloy is stable against phase separation into an  $\alpha$ -Si and an  $\alpha$ -C region, as discussed previously, and in agreement with experimental observations.<sup>46,51</sup>

Quite interestingly, a careful analysis (see Table I) shows that a fourfold carbon atom has, on average, about three silicon and one carbon atoms as nearest neighbors. On the other hand, the number of silicon and carbon neighbors of a threefold carbon atom are approximately equal. This suggests that most of the ordering arises from fourfold carbon atoms, and that in a tetrahedral network ordering will be maximized. As a check of this assumption, it is proper to look at the energetics of the “tetrahedral component” of the sample, that is, energies of bonds between tetrahedral atoms only. Indeed, a similar analysis as above results in  $V_{\text{Si-Si}} \simeq -2.2$  eV,  $V_{\text{C-C}} \simeq -3.68$  eV, and  $V_{\text{Si-C}} \simeq -3.10$  eV, which gives  $\Delta V_{\text{Si-C}} \simeq -0.16$  eV (or  $-0.32$  eV/atom), very close to the crystalline ZB value. This observation might be relat-

TABLE IV. Calculated equilibrium lattice constant  $\alpha_{\text{eq}}$ , isotropic bulk modulus  $B_0$ , and cohesive energy per atom  $E$ , for  $\alpha$ -Si, evaporated amorphous carbon *e*-C, diamondlike amorphous carbon *d*-C, stoichiometric  $\alpha$ -SiC, and ZB *c*-SiC. We distinguish between metastable,  $sp^3$ -rich *d*-C and the stable,  $sp^2$ -rich phase of *d*-C. See Ref. 15.

	$\alpha$ Si	<i>e</i> -C	<i>d</i> -C	$\alpha$ -SiC	<i>c</i> -SiC
$\alpha_{\text{eq}}(\text{\AA})$	$\sim 5.48$	$\sim 4.3$	3.7–3.8	$\sim 4.6$	4.32
$B_0$ (Mbar)	0.95	2.3	4.2–3.9	2.45	2.2
$-E$ (eV)	$\sim 4.4$	$\sim 6.9$	6.75–6.9	$\sim 5.75$	6.34

ed to indications for enhanced ordering in hydrogenated samples,<sup>48</sup> through the notion that hydrogen promotes fourfold carbon coordination.

Bond-energy distributions for the stoichiometric liquid sample are shown in Fig. 10(c). All distributions are very broad because of high- $T$  fluctuations. This makes the above analysis not as easily applicable. However, we could rather safely and within some error bars take the average bond energies to be  $V_{\text{Si-Si}} - 1.3$  eV,  $V_{\text{Si-C}} - 2.6$  eV, and  $V_{\text{C-C}} - 3.85$  eV, giving a very small value for  $\Delta V_{\text{Si-C}}$  ( $\sim -0.02$  eV), and indicating the randomness of the system. Again, I stress that this is just a rough estimate of  $\Delta V_{\text{Si-C}}$ , possibly the result should be given as an absolute value,  $|0.02|$  eV.

Finally, I would like to make an estimate of the compressibility of the amorphous alloys. For this purpose, we can define an isotropic, equilibrium bulk modulus for the amorphous phase, as is done in previous work on diamondlike amorphous carbon,<sup>15</sup> by analogy with the crystalline state and considering a uniform expansion (compression) of the system,

$$B_0 = V(d^2E/dV^2)_{V=V_0}, \quad (5)$$

where  $V$  is the volume,  $V_0$  the equilibrium volume, and  $E$  is the total energy of the cell. Values for  $B_0$  can be obtained by fitting calculated points of total energy versus volume to the Murnaghan’s equation of state for solids,<sup>63</sup> and they are listed in Table IV.  $\alpha$ -Si has a  $B_0$  slightly less than the crystalline value (0.99 Mbar). The diamondlike phases of  $\alpha$ -C have bulk moduli comparable with that of diamond (4.4 Mbars with this potential), while *e*-C takes a much lower value. I find an average value for the bulk modulus of stoichiometric  $\alpha$ -SiC (average over different samples) of  $\sim 2.45$  Mbars, which is larger than the  $B_0$  of ZB *c*-SiC. This can be explained by noting that the Si—C bond is softer than the average of Si—Si and C—C bonds since  $B_{\text{Si-C}} (=2.2) < 0.5[B_{\text{Si}} + B_{\text{C}}] (=2.7)$ . Introduction of homopolar bonds (especially diamondlike C—C bonds) then, in the amorphous phase, results in increased stiffness and a larger value for the bulk modulus.

## V. CONCLUSIONS

I have carried out extensive Monte Carlo simulations, within the empirical potential approach, in order to model the structure and energetics of disordered phases (amorphous and liquid) of silicon-carbon alloys and make a comparative study of them, with emphasis on the specification of short-range order.

The outstanding feature of the computer-generated amorphous samples is that homopolar bonds and threefold carbon coordination are an important ingredient in the description of these alloys. Therefore, the amorphous network deviates from an ideal tetrahedral geometry, as that proposed by the Polk model. This is more acute in carbon-rich samples. The threefold carbon geometries are not defective sites (dangling bonds), but they are of graphitelike nature, as bond angles and bond lengths confirm. While diamondlike homopolar (C—C) bonds

exist in carbon-centered tetrahedra, graphitelike bonding is rather associated with threefold carbon coordination, in analogy with observations in hydrogenated amorphous carbon.

The structure of the liquid alloys is even more complex than in the amorphous alloys. The competition among Si and C to impose their own favorable liquid structure seems to have been "won" by C. The resulting open structure forces Si to assume a coordination much lower than in the elemental system (*l*-Si), enhancing in this way the tetrahedral order and covalent bonding which persist in the liquid. Under pressure, silicon coordination rapidly increases but carbon coordination does not exceed four even at 1-Mbar pressure. At this pressure, pure *l*-C is less dense than diamond, indicating a positive slope of the diamond melting line in the phase diagram of carbon.

The simulations also reveal important information about chemical ordering in the disordered phases. It is found that the amorphous samples have a significant degree of ordering, although far from the maximum possible value. On the contrary, the distribution of atoms in the liquid is random, indicating that there is a gradual de-

crease of ordering from the solid (complete) to the liquid (zero). This is related to the weakening of the Si—C bond in the disordered environment. Insight into this effect is accomplished by decomposing the total energy of the system into bond energies. In a similar fashion, and by considering an "enthalpy of formation" of the amorphous phase, its stability against phase separation is explained. Finally, the compressibility of the amorphous alloys is examined by introducing an isotropic bulk modulus for the amorphous phase. It is found that stoichiometric  $\alpha$ -SiC has a bulk modulus somewhat larger than ZB *c*-SiC, due to the presence of homopolar bonds, whose average is stiffer than the Si—C bond.

A natural extension of this work is the investigation of the electronic (optical) properties of these alloys. Of particular interest is the effect on the band gaps and density of states of the amorphous alloys due to homopolar bonding and threefold coordination. Toward this goal, *ab initio* pseudopotential supercell calculations [within the local-density-approximation (LDA) formalism] on appropriate configurations are presently being carried out.<sup>54</sup>

- <sup>1</sup>G. Lucovsky and T. M. Hayes, in *Amorphous Semiconductors*, edited by M. H. Brodsky (Springer-Verlag, Berlin, 1979), Vol. 36, p. 215.
- <sup>2</sup>D. E. Polk, *J. Non-Cryst. Solids* **5**, 365 (1971).
- <sup>3</sup>D. E. Polk and D. S. Boudreaux, *Phys. Rev. Lett.* **31**, 92 (1973).
- <sup>4</sup>D. Turnbull and D. E. Polk, *J. Non-Cryst. Solids* **8-10**, 19 (1972).
- <sup>5</sup>N. J. Shevchik and W. Paul, *J. Non-Cryst. Solids* **8-10**, 381 (1972).
- <sup>6</sup>D. Henderson and F. Herman, *J. Non-Cryst. Solids* **8-10**, 359 (1972).
- <sup>7</sup>J. D. Joannopoulos and M. L. Cohen, in *Solid State Physics*, edited by H. Ehrenreich, F. Seitz, and D. Turnbull (Academic, New York, 1976), Vol. 31, p. 71.
- <sup>8</sup>S. T. Pantelides, *Phys. Rev. Lett.* **57**, 2979 (1986).
- <sup>9</sup>J. Robertson, *Adv. Phys.* **35**, 317 (1986), and references therein.
- <sup>10</sup>F. Li and J. S. Lannin, *Phys. Rev. Lett.* **65**, 1905 (1990).
- <sup>11</sup>J. Tersoff, *Phys. Rev. Lett.* **61**, 2879 (1988).
- <sup>12</sup>G. Galli, R. M. Martin, R. Car, and M. Parinello, *Phys. Rev. Lett.* **62**, 555 (1989); *Phys. Rev. B* **42**, 7470 (1990).
- <sup>13</sup>D. R. McKenzie, D. Muller, and B. A. Pailthorpe, *Phys. Rev. Lett.* **67**, 733 (1991).
- <sup>14</sup>P. H. Gaskell, A. Saeed, P. Chieux, and D. R. McKenzie, *Phys. Rev. Lett.* **67**, 1286 (1991).
- <sup>15</sup>P. C. Kelires, *Phys. Rev. Lett.* **68**, 1854 (1992).
- <sup>16</sup>C. Gao, Y. Wang, A. Ritter, and J. Dennison, *Phys. Rev. Lett.* **62**, 945 (1989).
- <sup>17</sup>M. A. Tamor and C. H. Wu, *J. Appl. Phys.* **67**, 1007 (1990).
- <sup>18</sup>D. Wagman, W. Evans, I. Hallow, V. Parker, S. Bailey, and R. Schumm, in *Selected Values of Chemical Thermodynamic Properties, Tables for the First Thirty-Four Elements in the Standard Order of Arrangement*, Natl. Bur. Stand. (U.S.) No. 270 (U.S. GPO, Washington, DC, 1968).
- <sup>19</sup>J. L. Martins and A. Zunger, *Phys. Rev. Lett.* **56**, 1400 (1986); *J. Mater. Res.* **1**, 523 (1986).
- <sup>20</sup>K. J. Chang and M. L. Cohen, *Phys. Rev. B* **35**, 8196 (1987).
- <sup>21</sup>P. J. H. Denteneer and W. van Haeringen, *Phys. Rev. B* **33**, 2831 (1986).
- <sup>22</sup>P. C. Kelires and J. Tersoff, *Phys. Rev. Lett.* **63**, 1164 (1989).
- <sup>23</sup>A. Qteish and R. Resta, *Phys. Rev. B* **37**, 1308 (1988); **37**, 6983 (1988).
- <sup>24</sup>S. de Gironcoli, P. Giannozzi, and S. Baroni, *Phys. Rev. Lett.* **66**, 2116 (1991).
- <sup>25</sup>Y. Waseda and K. Suzuki, *Z. Phys. B* **20**, 339 (1975).
- <sup>26</sup>J. Heremans, C. H. Olk, G. L. Eesley, J. Steinbeck, and G. Dresselhaus, *Phys. Rev. Lett.* **60**, 453 (1988).
- <sup>27</sup>G. Galli, R. M. Martin, R. Car, and M. Parinello, *Phys. Rev. Lett.* **63**, 988 (1989); *Phys. Rev. B* **42**, 7470 (1990).
- <sup>28</sup>Y. Waseda, *The Structure of Non-Crystalline Materials; Liquids and Amorphous Solids* (McGraw-Hill, New York, 1980).
- <sup>29</sup>H. R. Leider, O. H. Krikorian, and D. A. Young, *Carbon* **11**, 555 (1973); D. M. Haaland, *ibid.* **14**, 357 (1976).
- <sup>30</sup>P. C. Kelires, *Europhys. Lett.* **14**, 43 (1991).
- <sup>31</sup>P. C. Kelires, *Phys. Rev. B* **44**, 5336 (1991).
- <sup>32</sup>F. H. Stillinger and T. W. Weber, *Phys. Rev. B* **31**, 5262 (1985).
- <sup>33</sup>J. Tersoff, *Phys. Rev. Lett.* **56**, 632 (1986); *Phys. Rev. B* **37**, 6991 (1988).
- <sup>34</sup>J. Tersoff, *Phys. Rev. B* **38**, 9902 (1988).
- <sup>35</sup>J. Tersoff, *Phys. Rev. B* **39**, 5566 (1989).
- <sup>36</sup>R. Biswas and D. R. Hamann, *Phys. Rev. Lett.* **55**, 2001 (1985); *Phys. Rev. B* **36**, 6434 (1987).
- <sup>37</sup>J. R. Chelikovsky, J. C. Philips, M. Kamal, and M. Strauss, *Phys. Rev. Lett.* **62**, 292 (1989); J. R. Chelikovsky and J. C. Philips, *ibid.* **63**, 1653 (1989).
- <sup>38</sup>R. Car and M. Parinello, *Phys. Rev. Lett.* **55**, 2471 (1985).
- <sup>39</sup>Y. Tawada, K. Tsuji, M. Kondo, H. Okamoto, and Y. Hamakawa, *J. Appl. Phys.* **53**, 5273 (1982).
- <sup>40</sup>F. Fujimoto *et al.*, *Jpn. J. Appl. Phys.* **23**, 810 (1984).
- <sup>41</sup>R. Könenkamp, *Phys. Rev. B* **36**, 2938 (1987).
- <sup>42</sup>Y. Catherine and G. Turban, *Thin Solid Films* **60**, 193 (1979).
- <sup>43</sup>D. A. Anderson and W. E. Spear, *Philos. Mag.* **35**, 1 (1977).
- <sup>44</sup>T. Shimada, Y. Katayama, and K. F. Komatsubara, *J. Appl.*

- Phys. **50**, 5530 (1979).
- <sup>45</sup>A. Kaloyeros, R. Rizk, and J. Woodhouse, Phys. Rev. B **38**, 13 099 (1988).
- <sup>46</sup>M. Gorman and S. A. Solin, Solid State Commun. **15**, 761 (1974).
- <sup>47</sup>D. R. McKenzie, S. D. Berger, and L. M. Brown, Solid State Commun. **59**, 325 (1986).
- <sup>48</sup>J. Tafto and F. J. Kampas, Appl. Phys. Lett. **46**, 949 (1985).
- <sup>49</sup>F. A. Fagen, in *Amorphous and Liquid Semiconductors*, edited by J. Stuke and W. Brenig (Taylor & Francis, London, 1974), p. 601.
- <sup>50</sup>A. Sproul, D. R. McKenzie, and D. J. H. Cockayne, Philos. Mag. B **54**, 113 (1986).
- <sup>51</sup>K. Mui, D. K. Basa, F. W. Smith, and R. Corderman, Phys. Rev. B **35**, 8089 (1987).
- <sup>52</sup>K. Mui and F. W. Smith, Phys. Rev. B **35**, 8080 (1987).
- <sup>53</sup>P. C. Kelires and J. Tersoff, Phys. Rev. Lett. **61**, 562 (1988).
- <sup>54</sup>P. C. Kelires and P. J. H. Denteneer (unpublished).
- <sup>55</sup>F. Finocchi, G. Galli, M. Parinello, and C. Bertoni, J. Non-Cryst. Solids **137-138**, 153 (1991).
- <sup>56</sup>C. Meneghini, S. Pascarelli, F. Boscherini, S. Mobilio, and F. Evangelisti, J. Non-Cryst. Solids **137-138**, 75 (1991).
- <sup>57</sup>I. Stich, R. Car, and M. Parinello, Phys. Rev. Lett. **63**, 2240 (1989).
- <sup>58</sup>G. Galli, R. M. Martin, R. Car, and M. Parinello, Science **250**, 1547 (1990).
- <sup>59</sup>F. P. Bundy, Physica A **156**, 169 (1989).
- <sup>60</sup>J. W. Shaner, J. M. Brown, C. A. Swenson, and R. G. McQueen, J. Phys. (Paris) Colloq. **44**, C8-235 (1984).
- <sup>61</sup>A. C. Mitchell, J. W. Shaner, and R. N. Keller, Physica **139**, 386 (1986).
- <sup>62</sup>J. S. Dickey, W. A. Basset, J. M. Bird, and M. S. Weathers, Geology **11**, 219 (1983).
- <sup>63</sup>F. F. Murnaghan, Proc. Natl. Acad. Sci. U.S.A. **30**, 244 (1944).